JOURNAL OF SOLID STATE CHEMISTRY 29, 181–190 (1979)

A Neutron Diffraction Study on the Intercalation of Deuteropyridine into Tantalumdisulfide

C. RIEKEL

Institut Laue Langevin, B.P. 156X, 38042 Grenoble Cédex, France

AND C. O. FISCHER

Hahn–Meitner–Institut, Glienicker Strasse 100, D1000 Berlin 39, West Germany

Received July 6, 1977; in revised form October 5, 1978

The intercalation of C_5D_5N into the lattice of 2H–TaS_2 was followed by neutron powder diffraction using deuteropyridine as liquid phase. Disordered second-stage nuclei were found to initiate the reaction. Model calculations established that the nuclei contain about 30% first-stage layers and that the pyridine orientations are identical in the first- and second-stage compounds. Tracer exchange measurements indicate two pyridine fractions.

Introduction

A basic problem in the study of heterogeneous equilibria involving gas/solid or gas/liquid interfaces is the description of the structure of the solid phase at any time during the reaction. It has recently been shown for the system TaS_2/ND_3^{gas} (*1*) that neutron diffraction has some advantages over X-ray or electron diffraction due to: (i) the low absorption of both sample container and cryostat for neutrons, and (ii) the high scattering contribution of the intercalated molecules. In this paper the method is extended to a heterogeneous reaction involving solid/liquid interfaces.

The intercalation of pyridine into 2H–TaS_2 according to

$$2H\text{–}TaS_2^{solid} + 0.5\ C_5H_5N^{liq} \rightarrow TaS_2(C_5H_5N)_{0.5}^{solid} \qquad (1)$$

leads to a crystalline product (*2, 3*), the formation and structure of which are not well known. X-Ray (*2, 3*) and electron microscopy (*4*) data show that $TaS_2(C_5H_5N)_{0.5}$ is a first-stage compound with pyridine intercalated into every van der Waals gap. The space group was found from X-ray data to be $P6_3/mmc$ with two formula units per unit cell and hexagonal axes $a = 3.32_7$ Å, $c = 23.7$ Å (*3*), but electron microscopy data (*3*) indicate a much larger unit cell in *a* and *b*.

Several models for the pyridine orientation have been proposed from lattice expansion, X-ray, NMR, and neutron diffraction studies (*3, 5–7*) on $TaS_2(C_5H_5N)_{0.5}$ and related compounds.

Structural data indicate that the pyridine ring is oriented normal to the TaS_2 slabs but with the nitrogen atom midway between the TaS_2 slabs as in $NbS_2(C_5H_5N)_{0.5}$ [Ref. (*7*); and see below]. The reason for this orientation is not clear. Likewise, in $TaS_2 \cdot NH_3$ electronic (*6*) and ionic (*8*) stabilization models have been proposed to explain the interaction of NH_3 with TaS_2.

A second-stage compound, TaS_2-$(C_5H_5N)_{0.25}$, of unknown pyridine orien-

0022-4596/79/080181-10$02.00/0

tation, has been described (*2*) and electron microscopic evidence (*4*) indicates that pyridine is intercalated into every other van der Waals gap although no pure compound was found, due to the presence of additional first-stage regions. Thus one possible formulation for the idealized reaction is

$$2H\text{-}TaS_2^{solid} + 0.25\ C_5H_5N^{liq} \rightarrow TaS_2(C_5H_5N)_{0.25}^{solid}, \quad (2a)$$

$$TaS_2(C_5H_5N)_{0.25}^{solid} + 0.25\ C_5H_5N^{liq} \rightarrow TaS_2(C_5H_5N)_{0.5}^{solid}. \quad (2b)$$

Experimental Details

2H–TaS_2 was prepared as described elsewhere (*1*). The mean particle size obtained by sieving was about 0.1 mm. The sample (19.7 mmole) was contained in a quartz tube of diameter 10 mm which was connected to a high-vacuum line ($P_{min}^{pump} < 10^{-6}$ Torr). A vanadium resistance element heated the quartz tube. Temperature control was accurate within ±1°C.[1]

The D1B diffractometer and the data evaluation have been described elsewhere (*1*). The instrument was calibrated by measuring a KCl standard. Spectra were taken at a wavelength of 2.4 Å over a range of 2.55 to 82.55° (2θ), although the effective cutoff was at about 5° (2θ) due to the geometrical constraints of the furnace. Spectra of 3 min each were taken. The dead time between two consecutive spectra was about 2 sec. A total of 170 spectra were taken. Only the quartz background, measured at the temperature of the reaction (99°C), was subtracted from the raw data. This subtraction introduces some error, as the base line of the spectrum becomes negative due to self-shielding by absorption and scattering. As this affects all spectra during the reaction almost equally it can thus be neglected. The spectrum of the unreacted powder showed only the peaks due to 2H–TaS_2. In accordance with the literature reflections with $h - k \neq 3n$ were found to be broadened (*9*).

The experiment was started by injecting 5 ml of deuteropyridine through a rubber membrane into the preheated sample container; helium at atmospheric pressure was admitted and the container was then closed by a high-vacuum tap. The injection of the liquid coincided with the start of a spectrum. From the measurement of the lattice spacing of the (002) reflection of 2H–TaS_2 it is inferred that the time for thermal equilibration was less than 3 min. The liquid deuteropyridine increased the background by about factor 2 and introduced a broad peak centered at about 30° (2θ).[2] Gaussian profiles were fitted to the reflections as indicated in Ref. (*1*).

Results and Discussion

For the quantitative calculation of the intensity distribution along c^* (see below) only the orientation of the pyridine ring relative to the TaS_2 slabs has to be known. 2H–TaS_2 (*9*) and 2H–NbS_2 (*10*) are isotypic and it is assumed that the nitrogen lone pair is parallel to the slabs both in $TaS_2(C_5D_5N)_{6.5}$ and $NbS_2(C_5D_5N)_{0.5}$ since the relative intensities of the (00*l*) series are identical within the accuracy of the measurement (Figs. 1a, b). This agrees with model calculations for two possible ring orientations, which show large differences (Figs. 2a and b). There is no indication from the (00*l*) series after prolonged heating to 99°C and pumping to 10^{-6} Torr that the pyridine ring changes its orientation. A slight loss of pyridine may be indicated by the fact that the (002) deviates somewhat from a Gaussian profile at the tails, but no satellites as for

[1] The transmission of quartz tube + powder + liquid deuteropyridine at a wavelength of 2.4 Å is about 75%.

[2] Deuteropyridine was used to avoid the high incoherent background of hydrogen. Both deuteropyridine (Saclay 99%) and pyridine (see footnote 4) were distilled over P_2O_5.

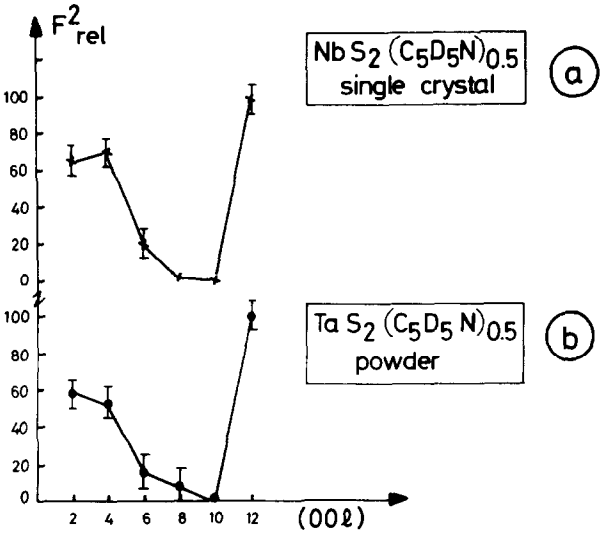

FIG. 1. (a) F^2_{rel} values of (00l) series from $NbS_2(C_5D_5N)_{0.5}$ single crystal (*7*). (b) F^2_{rel} values of (00l) series from $TaS_2(C_5D_5N)_{0.5}$ powder [scaled to (0012); $F^2_{rel} = 100$].

partially decomposed H_xTaS_2 (*11*) or $TaS_2(N_2H_4)_{1-x}$ (*12*) were resolved. The intensity of the (002) peak of 2H–TaS_2 has been plotted as a function of time in Fig. 3. As the peak positions of the (002) reflection of 2H–TaS_2 and the (004) of the first-stage compound coincide, the intensity never decreases to zero, but there is a certain incubation period before the influence of the (004) manifests itself as an increase in intensity. The rising part of the curve has a sigmoidal shape typical of a cooperative reaction, and nucleation effects may be expected.

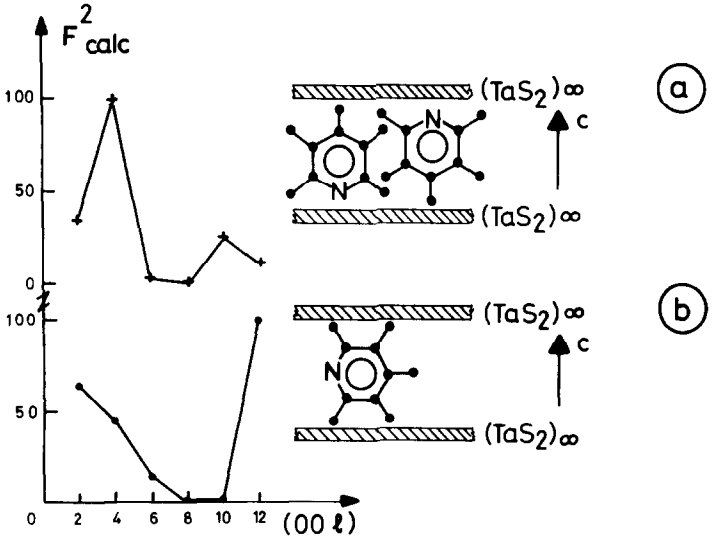

FIG. 2. Model calculations for $TaS_2(C_5D_5N)_{0.5}$. (a) Lone-pair electrons toward the slabs (scaled to (004); $F^2_{calc} = 100$). Note that maximum overlap of aromatic rings was assumed. (b) Lone-pair electrons parallel to the slabs [scaled to (0012); $F^2_{calc} = 100$].

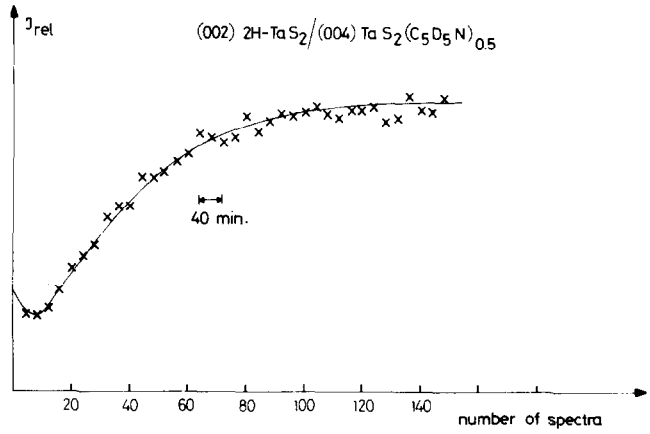

FIG. 3. Change in relative intensity of the (002) peak of 2H–TaS_2 during intercalation.

An additional spectrum (Fig. 4) taken 125 min after the pyridine injection shows two new peaks, both considerably broadened, one at $7.9°_1$ (2θ) $A1$ and another slight hump at ~15° (2θ) $A2$. $A1$ is quite close to the position calculated for a second-stage compound, and constant in position during the reaction.[3] As no additional peaks at smaller angles or an increase of the background were found, it is assumed that the reaction starts with the formation of the second-stage compound which is transformed into the first-stage compound. The maximum in second-stage formation corresponds to the turning point of the sigmoidal curve of first-stage formation (Fig. 5).

The broadening of the $A1$ peak is assumed to be due to disorder in the nuclei and not to a particle size effect. Arguments for a rapid growth of the intercalated phase can be found in Ref. (*12*). Furthermore, the (002) of the first-stage compound shows only instrumental broadening.

[3] A $2n$ extinction rule was also assumed for the ($00l$) reflections of the second-stage compound. The repeat unit of the second-stage compound ($c = 36.3$ Å) at 99°C may be obtained from the (002) of 2H-TaS_2 ($d = 6.0_8$ Å) and the (002) of $TaS_2(C_5D_5N)_{0.5}$ ($d = 12.0_5$ Å) (Fig. 6; note that the c-values are twice the values for the identity periods shown). The dimension and orientation of deuteropyridine are from Ref. (*7*).

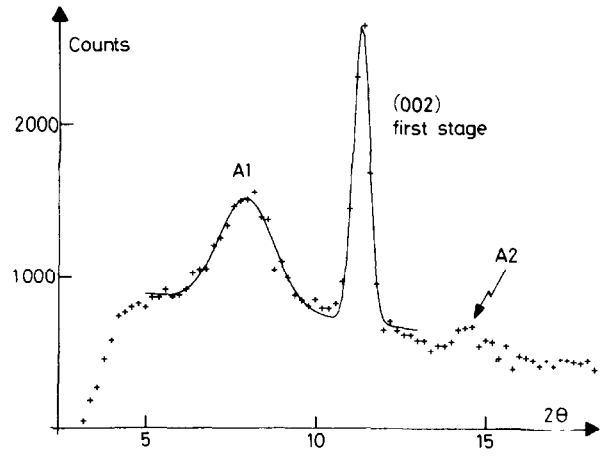

FIG. 4. $A1$ and $A2$ peaks at 125 min after the start of intercalation.

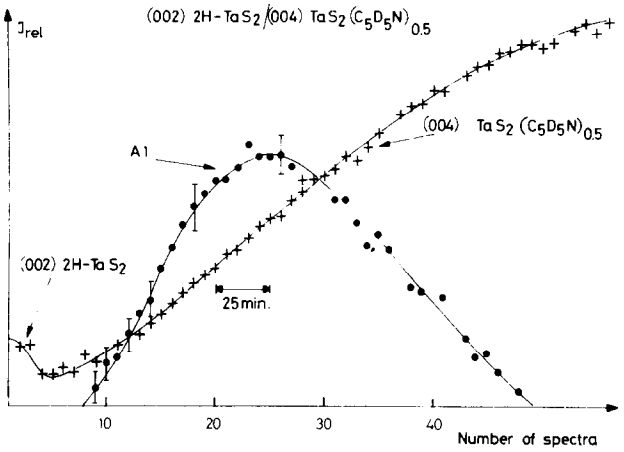

FIG. 5. Change in relative intensity of the (002) peak of 2H–TaS_2 and the $A1$ reflection.

X-Ray diffraction patterns of disordered graphite/$FeCl_3$ compounds may be analyzed by assuming a statistical mixture of n-stage layer packets. High-resolution electron microscopic data on partly decomposed first-stage graphite/$FeCl_3$ compounds support this model (*15*). A theory has been developed which is capable of describing the observed intensity pattern for such disordered compounds along c^* in a quantitative way (*13, 14*). Several assumptions will be made, to apply this theory to the dynamical situation.

1. All nuclei are composed of statistical sequences of m- and $(m+1)$st stage layer packets ($m=0$ corresponds to a TaS_2 slab, $m=1$ to a first-stage layer packet, i.e., TaS_2 slab + pyridine layer) and $m=2$ to a second-stage layer packet. More complicated models will be considered only when neither model gives a satisfactory correspondence between observed and calculated spectra. The basic packets are shown in Fig. 6 (bold lines).

2. The $A1$ peak is sufficiently close to the calculated (002) peak position of a second-stage compound that one need consider only admixtures of one additional layer packet to the second-stage compound. Two models will be considered: (a) Model I, containing second- and first-stage packets; and (b) Model II, containing second-stage and TaS_2 packets.

Another simple model containing first-stage and TaS_2 packets can be excluded, as

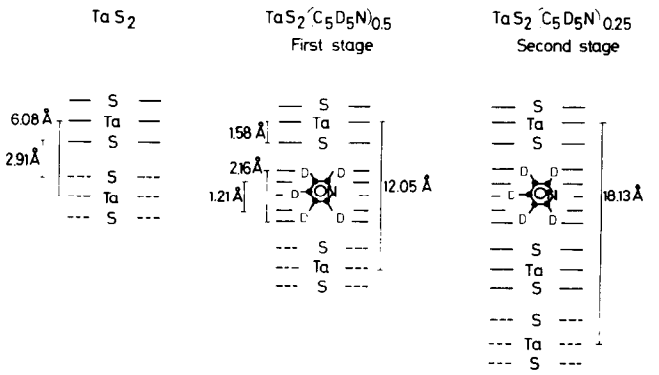

FIG. 6. Structural units of TaS_2, $TaS_2(C_5D_5N)_{0.5}$, and $TaS_2(C_5D_5N)_{0.25}$.

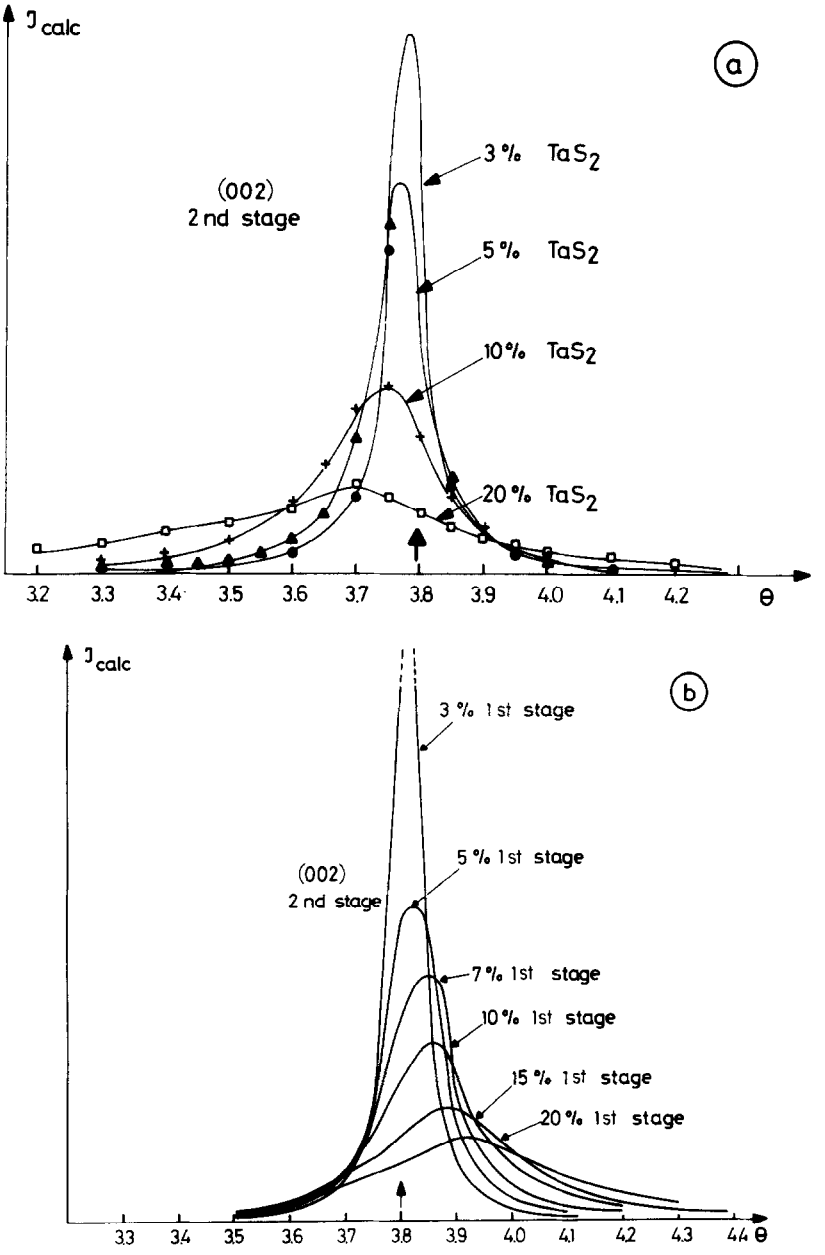

FIG. 7. (a) Effect of admixture of TaS_2 packets to second-stage packets on the (002) reflection. (b) Effect of admixture of $TaS_2(C_5D_5N)_{0.5}$ packets to second-stage packets on the (002) reflection.

the peak position for the disordered compound will lie between the peak positions of the two pure compounds and will not fall in the region where $A1$ is observed.

3. The packing density of pyridine in the second-stage compound is identical to that of the first-stage compound.

The intensity distribution along c^* was calculated for these two models. It was

always found that the calculated intensity of the second-stage (004) reflection decreased very rapidly when other stages were admixed. This is also observed experimentally, and the $A2$ peak at about 15° (2θ) in Fig. 4 corresponds to the remnants of the (004) peak. No other higher-order reflections of reasonable intensity are present.

The appropriate model should fulfill the condition that both calculated full width at half-height (FWHH) and peak position correspond to the observed values. The influence of disorder on the second-stage (002) reflection for the different models is shown in Figs. 7a and b. The analysis shows that only Model I, i.e., packets of first- and second-stage layers, fits the peak position and FWHH of the $A1$ reflection reasonably well. Model II can be excluded as increasing disorder (admixture of TaS_2 layers) shifts the peak position to smaller angles, contrary to the observed $A1$ position.

In Table I the values of the peak position and FWHH of the $A1$ reflection at the point of its maximum intensity are compared with the best-fitting values of Model I. This corresponds to about 70% second-stage layers and 30% first-stage layers. The close coincidence of calculated and observed values suggests that our model is correct.

TABLE I

VALUES OF FWHH AND PEAK POSITION OF $A1$ AT MAXIMUM INTENSITY

FWHH (002) °(2θ)	
Calculated	1.35
Observed	1.3_2
Peak position °(2θ)	
Calculated	8.00
Observed	7.9_1

Electron microscopic results likewise show that the second-stage compound is characteristically disordered and contains first-stage regions (*4*). In Fig. 8 the total spectrum calculated for this layer sequence is shown, and the small broad hump at 16° (2θ) corresponds roughly to the observed value in Fig. 4. The calculated reflection at 32° (2θ) is not observed as the deuteropyridine has a strong peak in this region. The model could have been further refined by taking into account the Debye–Waller factors of TaS_2 and of the interrelate layer.

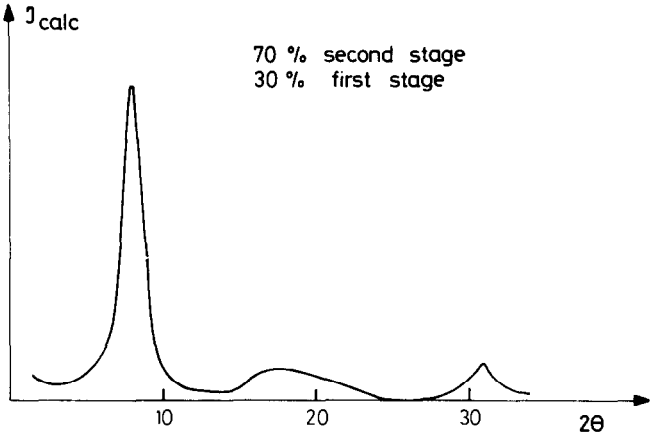

FIG. 8. Calculated spectrum assuming 70% second-stage and 30% first-stage layers.

The description is still somewhat idealized, as the broadening of the $A1$ peak increases over the reaction period (Fig. 9). This would correspond in terms of the model to a change in the relative amounts of first- and second-stage layers of ~5% which would not be evident from an analysis of the observed peak position. To characterize the first-stage compound further tracer exchange measurements according to

$$TaS_2(C_5H_5N)_{0.5} + 0.5C_5D_5N \rightarrow TaS_2(C_5D_5N)_{0.5} + 0.5C_5H_5N \quad (3)$$

were done on a freshly prepared $TaS_2(C_5H_5N)_{0.5}$ sample. The exchange process may be readily followed as the (002) and (004) intensities change considerably upon isotope exchange. The calculated change is shown in Fig. 10 for the two (00l) reflections. From the velocity of exchange and the intensities of (002) and (004) at the end of the exchange two parameters should be accessible: (i) the ratio C_5H_5N/C_5D_5N at the end of the exchange; and (ii) a value for the pyridine mobility, provided that the rate-determining step is the diffusion within the layers.

No exchange was observed with gaseous C_5D_5N (room temperature to 100°C), which suggests that the interaction of pyridine with the basal plane plays a decisive role as for the TaS_2/NH_3 system (*16*). However, an exchange was observed for $T > 70$°C, when an excess of thermostatted deuteropyridine (~20 times the amount of pyridine intercalated) was injected into the reaction vessel.[4] The subsequent change in (002) and (004) intensities was monitored with the D1B multidetector. The ratio $J_{rel}^{(002)}/J_{rel}^{(004)}$ was found to be close to one when the intensities showed no more apparent change. Model calculations for various C_5H_5N/C_5D_5N ratios, shown in Fig. 10, suggest that about 50% of the pyridine molecules are exchanged, as the ratio $J_{calc}^{(002)}/J_{calc}^{(004)}$ is then close to one. Obviously

[4] No evidence for a first-order transition due to the onset of pyridine mobility has been found between room temperature and 100°C. Superlattice reflections due to the pyridine lattice (*7*) are present up to at least 80°C. Total cross-section measurements on $TaS_2(C_5H_5N)_{0.5}$ at the HMI Berlin with subthermal neutrons at a wavelength of 11 Å showed no step in the cross-section curve. A step was found, for example, for the first-order transition in NH_4 J at −13.5°C (*18*).

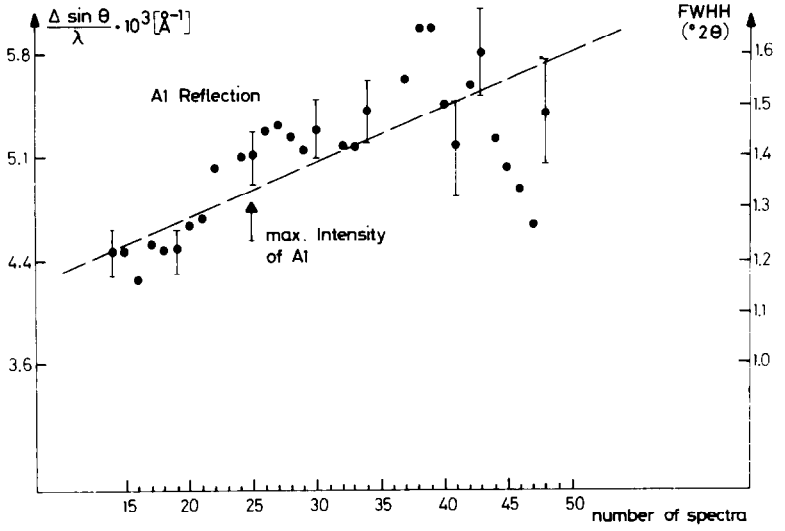

FIG. 9. Evolution of the full width at half-height of the $A1$ reflection.

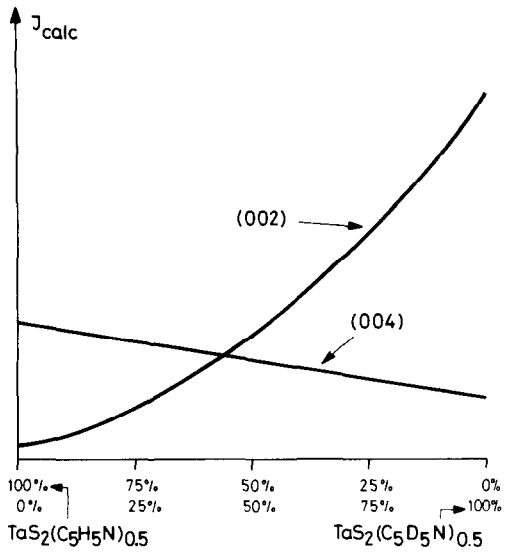

FIG. 10. Calculated intensities of (002) and (004) for $TaS_2(C_5H_5N)_x(C_5D_5N)_{0.5-x}$ $(0<x<0.5)$.

half of the pyridine molecules are more mobile than the other half. The formation of a two-phase material, resulting from the intercalation of pyridine into 2H-TaS_2, has already been suggested (*17*), and it is tempting to speculate that high-temperature deintercalation leads first to a loss of the more mobile fraction. At present we do not know whether two different $TaS_2(C_5H_5N)_{0.5}$ fractions or two differently bound pyridine fractions within each $TaS_2(C_5H_5N)_{0.5}$ crystallite are present. Some caution seems to be necessary when comparing different $TaS_2(C_5H_5N)_{0.5}$ samples, as we had to heat some TaS_2 samples with liquid pyridine in sealed glass tubes to 180°C to reach quantitative reaction. Obviously, the influence of stoichiometry and the presence of additional TaS_2 polymorphs are not well understood. A rough value for the macroscopic diffusion coefficient D^* may be derived from the half-time of exchange ($\tau_T^{1/2}$) which is 25 ± 5 min at 84°C. In first approximation Eq. (4) holds (*19, 20*).

$$0.5 \approx \frac{2A}{V}\left(\frac{D^* \cdot \tau_T^{1/2}}{\pi}\right)^{1/2}, \qquad (4)$$

where A is the area of crystallites in the direction of exchange and V is its volume. Assuming that the diffusion occurs near the boundaries between mosaic blocks which are $\sim 1\ \mu m \times (50\ \mu m)^2$ (*12*) we calculate $D^* = 6.10^{-9}\ cm^2/sec$ at 84°C.

Conclusion and Outlook

The heterogeneous chemical reaction of liquid deuteropyridine with 2H-TaS_2 has been examined by neutron powder diffractometry. A model for the nucleation phase has been suggested and evidence for two pyridine fractions of different mobilities was found. The experimental technique is applicable to many other heterogeneous reactions, and it is of interest to ask what the limits are in time resolution. With the present flux of $\sim 10^6\ N\ cm^{-2}\ sec^{-1}$ spectra taken in ~ 1 min will have ~5–10% statistical accuracy on the strongest peaks. Experimental details such as particle orientation play an important role and may modify the time resolution considerably.

By moving the multidetector to a beam of higher intensity or longer wavelength a considerable reduction in time resolution is possible. A time resolution of 43 msec/spectrum has recently been demonstrated for a quartz single crystal with a new multidetector system on the D2 instrument at the ILL at a wavelength of 1.7 Å and a flux of $10^8\ N\ cm^{-2}\ sec^{-1}$ (*21*).

References

1. C. RIEKEL AND R. SCHÖLLHORN, *Mater. Res. Bull.* **11**, 369 (1976).
2. F. R. GAMBLE, J. H. OSIECKI, M. CAIS, AND R. PISHARODY, *Science* **174**, 493 (1971).
3. G. S. PARRY, C. B. SCRUBY, AND P. M. WILLIAMS, *Phil. Mag.* **29**, No. 3, 601 (1974).
4. H. FERNÁNDEZ-MORÁN, MITSUO OHSTUKI, AKEMI HIBINO, AND C. HOUGH, *Science* **174**, 498 (1971).
5. R. SCHÖLLHORN AND A. WEISS, *Z. Naturforsch. B* **27**, 1275 (1972).

6. J. V. ACRIVOS, S. F. MAYER, AND T. H. GEBALLE, *in* "Electrons in Fluids" (J. JORTNER AND N. KESTNER, Eds.), p. 341, Springer-Verlag, Berlin (1973).
7. C. RIEKEL, D. HOHLWEIN, AND R. SCHÖLLHORN, *Chem. Commun.* 863 (1976).
8. R. SCHÖLLHORN AND H. D. ZAGEFKA, *Angew. Chem.* **89**, No. 3, 193 (1977).
9. F. JELLINEK, *J. Less-Common Metals* **4**, 9–15 (1962).
10. F. JELLINEK, G. BRAUER, AND H. MÜLLER, *Nature* **185**, 376 (1960).
11. C. J. WRIGHT, C. RIEKEL, R. SCHÖLLHORN, AND B. TOFIELD, *J. Solid State Chem.* **24**, 219 (1978).
12. J. V. ACRIVOS, C. DELIOS, AND H. KURASAKI, *Phil. Mag.* **34**, No. 6, 1047 (1976).
13. W. METZ AND D. HOHLWEIN, *Carbon* **12**, 87–96 (1975).
14. D. HOHLWEIN, Ph.D. Thesis, University of Hamburg (1972).
15. J. M. THOMAS, G. R. MILLWARD, N. C. DAVIES, AND E. LI. EVANS, *J. Chem. Soc. Dalton Trans.*, 2443 (1976).
16. J. V. ACRIVOS, C. DELIOS, N. Y. TOPSŒE, AND J. R. SALEM, *J. Phys. Chem.* **79**, No. 26, 3003 (1975).
17. A. H. THOMPSON, *Nature* **251**, 492 (1974).
18. J. J. RUSH, T. J. TAYLOR, AND W. W. HAVENS, *J. Chem. Phys.* **37**, 234 (1962).
19. R. M. BARRER AND B. E. F. FENDER, *J. Phys. Chem. Solids* **21**, 12–24 (1961).
20. C. REIKEL, *Solid State Commun.*, **28**, 385 (1978).
21. C. RIEKEL, P. CONVERT, J. JACOBE, AND R. KLESSE, to be published.